Supplement of Atmos. Chem. Phys., 15, 4077–4091, 2015
http://www.atmos-chem-phys.net/15/4077/2015/
doi:10.5194/acp-15-4077-2015-supplement

Atmospheric Chemistry and Physics
Open Access

Supplement of

Ice nucleation by water-soluble macromolecules

B. G. Pummer et al.

Correspondence to: B. G. Pummer (b.pummer@mpic.de)

S1 Theoretical considerations

S1.1 Macromolecules and solubility

Macromolecules are per definition molecules with a molecular mass of >10 kg/mol (Staudinger and Staudinger, 1954), which is equivalent to >10 kDa. In contrast to crystals or metals, which consist of subunits that are held together by non-covalent forces (e.g. ionic, metal or dipole bonds), each atom of a macromolecule is covalently bound to the rest of the molecule. Since covalent bonds are usually much stronger than non-covalent bonds, they stay intact in solution. In contrast, a sodium chloride crystal is broken down into single sodium cations and chloride anions and thereby loses its former structure. The variety of macromolecules ranges from inorganic (e.g. diamond, silicate) to organic (e.g. plastics) to biological (e.g. proteins, polysaccharides, sporopollenin, lignin) exponents.

Polymers are a subgroup of macromolecules, which are built up by a chain of covalently linked small molecules. Such a molecular chain will not stay linear, but will fold into a more compact form – especially if it contains hydrophobic elements in a hydrophilic surrounding or the other way round. This folding can be either random or in a well-defined manner. Proteins in their functional state usually have a very distinct folding. Protein chains that are not properly folded lack in most cases their functionality. Since the non-covalent forces holding the protein structure intact are usually weak, stress treatments lead to unfolding and therefore inactivation of the protein.

The solubility of a macromolecule depends on the chemistry of the macromolecule and the solvent. Based on the protein classification approach by T. B. Osborne (Osborne, 1910) biological matter is suspended and shaken in a certain solvent. Then the matter is centrifuged or filtrated off, thus removing particulate matter and yielding a transparent supernatant. Molecules that are extracted into the supernatant are considered to be soluble in that medium.

In the case of large molecules, it is disputable where to draw the line between solution and suspension. Per definition, a solution consists of a single phase, while a suspension consists of two phases with phase interfaces. If the particles sizes are close to the wavelength of visible light, a suspension shows light scattering, which makes it opaque. A solution, in contrast, shows neither light scattering, nor visible particles. Furthermore, a solution shows no phase separation

over time, while sedimentation or agglutination lead to a progressive phase separation in time. Additionally, solutions cannot be separated by centrifugation. From a molecular point of view, a molecule in solution is fully covered with an energetically favorable hydration shell.

S1.2 Basic physics of INA

At temperatures below the melting point (273.15 K at atmospheric pressure), ice is thermodynamically favored over liquid water. Nevertheless, the spontaneous freezing of liquid water that is supercooled below this point is statistically very unlikely, because the phase transition is kinetically hindered. To form ice, water molecules have to be arranged in a defined ice crystal structure instead of the more random orientation and translational degrees of freedom they have in a liquid. Due to energetic propitiousness, which comes from the crystallization energy, clusters of a few water molecules will tend to arrange in an ice-like structure in the liquid water body. These clusters, which are also known as ice embryos, however, are then ripped apart by their surface tension, so in supercooled water, there is equilibrium between formation and decay of ice embryos.

Crystallization energy is proportional to the volume of the ice embryo, and therefore to the radius cubed. In contrast surface tension is proportional to the surface, and therefore to the radius squared. The outcome of the battle between crystallization energy and surface tension depends on the value of the Gibbs Energy ΔG, which is therefore a function of the radius r (see Eq.(S1)), in other words the size of the water molecule cluster. $\Delta G(r)$ initially increases with r, then reaches a maximum ΔG^*, which is equivalent to the activation energy of the process (see Eq.(S2)). After that, ΔG strongly decreases with r. Once the critical radius r^* (see Eq.(S3)) is reached, meaning that the activation barrier ΔG^* is overcome, the ice embryo will grow unimpededly and subsequently catalyze the freezing of the entire supercooled body of water.

The critical ice embryo size in turn depends on the temperature, decreasing in size as the intensity of supercooling increases, or, in other words as the temperatures drop below 273.15 K. For example, 45000 arranged water molecules constitute the critical ice embryo size at 268 K, while only 70 are required at 233 K (Zachariassen and Kristiansen, 2000). Furthermore, the probability of forming a cluster decreases with its size. Therefore, freezing becomes very unlikely at higher temperatures (so far we take only water molecules into account). This situation

is the basis of why ultrapure water can be cooled down to temperatures about 235 K before it will eventually freeze. The manifestation of a critical ice embryo, which eventually leads to ice formation, is called ice nucleation. When only water molecules are involved, it is called homogeneous ice nucleation (see Fig. 1a).

$$\Delta G = 4\pi \cdot \gamma \cdot r^2 + \frac{4}{3}\pi \cdot \rho \cdot \Delta\mu \cdot r^3 \quad \text{(S1)}$$

$$\Delta G^* = \frac{16\pi \cdot \gamma^3}{3 \cdot \rho^2 \cdot (\Delta\mu)^2} \quad \text{(S2)}$$

$$r^* = -\frac{2 \cdot \gamma}{\rho \cdot \Delta\mu} \quad \text{(S3)}$$

ΔG…Gibbs energy, r…cluster radius, γ… surface free energy, ρ…bulk density, $\Delta\mu$…phase transition chemical potential, ΔG^*…activation energy, r^*…critical radius

The probability of freezing increases when water contains or comes in contact with structured surfaces that simulate ice and arrange water molecules in an ice-like manner. This stabilizes ice embryos, and therefore decreases the activation barrier in the manner of a catalyst. These ice-template structures are known as ice nucleators (INs) or ice nuclei, and the process they catalyze is known as heterogeneous ice nucleation (see Fig. 1b+c). The driving force of the arrangement of water molecules on IN surfaces is interaction between the partially charged ends of the water molecule and oppositely charged functional groups on the IN surface. This involves H-bonds between hydrogen atoms with partial positive charges and oxygen or nitrogen atoms with partial negative charges. Therefore, the IN has to carry functional groups at the proper position to be effective (Liou et al., 2000, Zachariassen and Kristiansen, 2000). In most cases only certain sections, which are known as “active sites”, participate in the INA, while the majority of the IN surface is inactive (Edwards et al., 1962, Katz, 1962).

The larger the active site of an IN, and the more fitting functional groups it carries, the more effective it stabilizes clusters, and so the higher the freezing temperature. Consequently, single molecules of low-molecular compounds cannot nucleate ice. In fact, soluble compounds consisting of very small molecules or ions, like salts, sugars or short-chained alcohols, cause a freezing point depression. However, if single molecules are very large, they can allocate enough active surface to be INs by themselves. Such ice nucleating macromolecules (INMs) are especially common among biological INs. Due to the same reason some low-molecular organic

compounds which do not induce ice formation in solution, can act as IN, if they are crystallized in layers of a certain arrangement (Fukuta, 1966).

S1.3 INA modes

Throughout the manuscript we present the physics of ice nucleation mainly with regard to immersion freezing where the IN is inside a cooling water droplet. But in fact, three more modes of ice nucleation are defined. Immersion freezing is the most-investigated mode, and is suspected to be the dominant ice formation mechanism in mixed-phase clouds (Ansmann et al., 2009, Wiacek et al., 2010, de Boer et al., 2011). The other modes are contact, deposition and condensation ice nucleation. Contact ice nucleation means that the IN collides with a supercooled droplet, which freezes on contact. Deposition ice nucleation is adsorption of water vapor on the IN surface as ice, and condensation ice nucleation is condensation of water vapor as liquid layer on the IN, which then freezes at the same temperature. Deposition ice nucleation is somewhat different, since the water molecules from the gas phase have to be arranged, while in the other modes freezing occurs in the liquid phase. Consequently, some particles that have shown ice nucleation activity (INA) in the other three modes are inactive in the deposition mode (Diehl et al., 2001, Diehl et al., 2002). Condensation and deposition mode depend additionally on atmospheric pressure and humidity, which play no role, if ice nucleation occurs in pre-existing droplets. For condensation mode activity, the IN additionally has to carry hygroscopic functional groups, which also make it an efficient cloud condensation nucleus (CCN). Since all four modes are theoretical models, they are permanently under discussion. Debates go so far as to question not only the real-life relevance, but also the existence itself of some modes. For example, one could claim that a condensation IN is consecutively acting as a CCN and an immersion IN (Fukuta and Schaller, 1982, Wex et al., 2014). In light of this debate we focus only on immersion freezing.

S1.4 Water activity

It is possible to view INA in the light of the water activity (a_w). The thermodynamic freezing and melting temperature of water (T_m), which is independent of insoluble INs, is a function of a_w. A

reduction of a_w due to the addition of solutes leads to a freezing point depression, as it is illustrated in Fig. S1. The effective freezing / ice nucleation temperature shows the same dependence on a_w, but is horizontally shifted relative to the $T_m(a_w)$-curve (Zobrist et al., 2008, Koop and Zobrist, 2009). The distance between the ice nucleation and melting curve at a given temperature is named Δa_w, which is the measure of the INA of a water sample. For example, for the homogeneous freezing on IN-free samples, Δa_w is about 0.31±0.02 (Koop et al., 2000, Koop and Zobrist, 2009). The addition of IN in the water leads to a horizontal shift of the ice nucleation curve towards the melting curve, or a reduction in Δa_w. In the experiment, a nucleation spectrum of a water droplet ensemble with given INA and a given a_w is like a vertical trajectory going through the phase diagram in Fig. S1 from top to bottom. Therefore, the ice nucleation temperature depends on both the present INs and a_w.

Instead of assigning a certain ice nucleation temperature to a sample, it is more accurate for stochastic, time-dependent INs to assign nucleation rate coefficients $J(T,a_w)$, which increase with decreasing T and increasing a_w (Knopf and Alpert, 2013). Therefore, one can add J contour lines to Fig. S1, which show the same shape as the thermodynamic and the homogeneous freezing curve (Koop et al., 2000, Attard et al., 2012, Knopf and Alpert, 2013). This means that from the thermodynamic freezing line to the homogeneous freezing line we have a gradient of increasing J. Accordingly, cooling is a steady increase in J. This makes J independent of the absolute freezing temperature, and therefore of the IN type.

S1.5 Motivation for expression of biological INMs

There are several theories addressing the question of why some organisms produce IN. Overall, it is proposed that INA is a form of adaption for survival or enhanced fitness in cold environments. More than 80% of the total biosphere volume is exposed to temperatures below 278 K, thriving either in the oceans or in frosty regions (Christner 2010). Also in temperate climate zones, temperatures can regularly drop below the freezing point. The formation of ice crystals can pierce cell walls and membranes, which leads to loss of cell fluids. Consequently, adaptations for either avoiding or managing freezing make sense for the many species that are exposed to such hostile conditions. The correlation between the INA of bacteria and the geographic latitude that was found by Schnell and Vali (1976) supports the idea of a selective

advantage for organisms with INA in cold environments. For the γ-Proteobacteria the gene for the BINM most likely originates from the common ancestor of this class of bacteria and therefore has been part of the genome of these organisms for at least 0.5 to 1.75 billion years (Morris et al., 2014). To be maintained for this length of time, the gene is likely to be under positive natural selection because it confers a fitness advantage. The possible advantages that have been proposed are:

(i) Nutrient mining (Lindow et al., 1982): Highly active INMs were mainly found in plant pathogenic species (bacteria, *Fusarium*, rust fungi) or in lichen. By inciting the growth of ice crystals, these organisms can essentially "dig" into the substrate on which they are growing (mainly plant tissues, but also rocks in the case of lichens), thereby acquiring nutrients.

(ii) Cryoprotection (Krog et al., 1979, Duman et al., 1992): The INA of plants and animals, but possibly also of lichens, is protective against frost injury. Ice growth in organisms is dangerous, because it ruptures the sensitive cell membranes thereby damaging or killing the cells. If the ice is formed on a less sensitive location, such as outside of the cells (e.g. in intercellular fluids), the danger of frost injury is far lower. Forming ice on the INMs prevents further ice formation at other places – partly because of the change in water activity, but also due to the release of crystallization heat, which prevents a further temperature decrease. This might explain why most known biological INMs are extracellular (see Table 1), and why they are active at such high temperatures, where the heat of fusion is sufficient to warm the cells to survivable temperatures.

(iii) Water reservoir (Kieft and Ahmadjian, 1989): Ice crystals might serve as water storage in cold and dry environments. The form stability of ice and its low vapor pressure reduce the potential loss of water in comparison to the loss from liquid water droplets.

(iv) Cloud seeding to assure deposition (Morris et al., 2008, 2013a, 2013b): The lifecycles of some species involve long distance dissemination that takes them up into clouds but where they will not proliferate unless they return to Earth's surface. Particles that attain cloud height are generally too small to deposit due to their own weight.

Therefore, they require means of active deposition, such as precipitation that forms from ice initiated in clouds via ice nucleation.

(v) Incidental (Lundheim 2002): In some cases, INA was detected where it cannot be explained by any reason. In this case, the INA might be an accidental property of a bioparticle that has another function in the organism. For example, the low density lipoproteins in human blood show INA, although their purpose lies in fat metabolism.

Advantages (i) and (ii) might be distinguishable by the freezing temperature (Duman et al., 1992): Since (i) demands ice formation as soon as possible, and the formation of few large ice crystals, such INMs are active at a very high temperature. On the other hand, type-(ii)-INMs are active at lower temperatures, only before other parts of the organism would start freezing. Furthermore, less efficient IN favor formation of smaller, less sharp and damaging ice crystals than those formed by type-(i)-INMs.

S1.6 Mineral dust IN

Apart from biological INMs, some types of mineral dust and soot have shown INA in different laboratory experiments (e.g. Murray et al., 2012), what might make them relevant for atmospheric ice formation.

Among mineral dust, potassium feldspar and fluorine phlogopite (a type of potassium micas) showed by far the highest INA (Shen et al., 1977, Atkinson et al., 2013, Augustin-Bauditz et al., 2014, Zolles et al., 2015). The reason for this higher accentuated activity compared to other closely related minerals is thought to be due to the potassium cations, whose hydration shell density matches that of ice. In contrast, the hydration shells of sodium and calcium ions are far tighter due to the higher ion charge density. So they likely disturb the ice-like water molecule arrangement, while potassium is neutral or supportive (Shen et al., 1977). It should be pointed out that this hypothesis is not valid for low molecular weight compounds. Soluble potassium salts (e.g. KCl, KNO_3, etc.) lead to a freezing point depression, as do salts with other cations. In the crystal lattice of feldspar the ions are fixed in a confined geometry that seems to match the ice crystal lattice. This probably causes the INA. Other ions with the same charge and the approximately same diameter, for example ammonium, might also have a favorable effect on the INA. It is interesting to note that several studies suggest that traces of ammonium contaminants

in silver iodine increase its INA (e.g. Corrin et al., 1964, Steele and Krebs, 1966, Bassett et al., 1970).

S2 Details about methods

S2.1 Molecular modeling

The insect antifreeze protein (AFP) from the beetle *Tenebrio molitor* was simulated (see Fig. 1c). The 8.4 kDa AFP is composed of 12-residue repeats and is stabilized by disulfide- bonds in the core of the protein. A defined structure of six parallel beta-sheets built up from the sequence TCT shows a high ordered surface to the water. The starting structure was taken from the *Protein Data Bank* (Liou et al., 2000), protonated with "prontonate3d" from the MOE2013.08 modeling package, and solvated in TIP4P-2005 water (Abascal and Vega, 2005) with 12 Å wall separation. Minimization and equilibration were performed according to Wallnoefer et al. (2010). Then 100 nanoseconds of NpT (isothermal and isobaric) molecular dynamics simulation at 220 K were recorded using an 8 Å cutoff for non-bonded interaction and the *Particle Mesh Ewald* algorithm for treating long-range electrostatics (Darden et al., 1993).

Water Analysis: Snapshots were taken every picosecond, and water density was estimated as described by Huber et al.(2013). Afterwards, the most likely water positions were extracted. During the simulation of 1EZG a very well structured first layer of water, which we colored blue, could be observed. Water less structured than the first layer was colored red.

S2.2 Size exclusion chromatography

High-purity water (18.2 MΩ·cm) was taken from an ELGA LabWater system (PURELAB Ultra, ELGA LabWater Global Operations, UK). Ammonium acetate (NH_4Ac; ≥ 98%, puriss p.a.), DL-dithiothreitol (DTT; > 99%), iodoacetamide (IAM; ≥ 99%), 2,2,2-trifluoroethanol (TFE; ≥ 99%, ReagentPlus), ammonium bicarbonate (NH_4HCO_3; ≥ 99%, ReagentPlus), Trypsin from porcine pancreas (proteomics grade) and protein standard mix (15–600 kDa) were obtained from Sigma Aldrich, Steinbach, Germany. Formic acid (FA; > 99%, for analysis) was from Acros Organics, Geel, Belgium. Guanidinium chloride was from Promega, Madison, WI, USA.

The HPLC-DAD system consisted of a binary pump (G1379B), an autosampler with thermostat (G1330B), a column thermostat (G1316B), and a photo-diode array detector (DAD; G1315C) from Agilent Technologies (Waldbronn, Germany). Chemstation software (Rev. B.03.01, Agilent) was used for system control and data analysis. A size exclusion column (Agilent Bio SEC-3, 300 Å, 4.6 x 150 mm, 3 µm particle size) with exclusion limits of 5 kDa to 1.25 MDa was used for chromatographic separation. 50 mM NH_4Ac in ultrapure water (pH 6.7) was used as the eluent. Isocratic analyses with a runtime of 10 min were performed at 303 K with a flow rate of 350 µL min^{-1}. After each measurement the column was flushed for 5 min with the same eluent before the next run. Absorbance was monitored at wavelengths of 220 and 280 nm. The sample injection volume was 40 µL. Sample fractions were collected at different retention time intervals corresponding to different molecular weight intervals as shown in Table S1. Molecular weights are calculated according to a protein standard mix with four calibration points ranging from 15 to 600 kDa. To get rid of the residues from the birch pollen extract, the column was cleaned after each work day with 6 M guanidinium chloride overnight, and then with pure water.

The protocol for the protein digestion was as follows: 5 µL of a 100 mM NH_4HCO_3 solution and 5 µL TFE were added to 100 µL of sample. Then 0.5 µL 200 mM DTT solution were added, the sample was briefly vortexed and then incubated for 1 h at 333 K to denature the proteins. After letting the sample cool to room temperature 2 µL of 200 mM IAM solution were added and the sample was allowed to stand for 1h in the dark (covered with aluminum foil) to alkylate the protein cysteine residues. The sample was allowed to stand for another hour in the dark after adding 0.5 µL 200 mM DTT solution to destroy excess IAM. Now 60 µL autoclaved water and 20 µL 100 mM NH_4HCO_3 solution were added to adjust the sample pH for digestion. Two microliters of 1 µg/µL Trypsin in 50 mM acetic acid was added and the sample was incubated at 310 K for 18 h. To stop the digestion 0.5 µL FA were added. The procedure for the treatment of samples and controls is given in Table 2.

References (Supplement)

Abascal, J. L. F., and Vega, C.: A general purpose model for the condensed phases of water: TIP4P/2005, J. Chem. Phys., 123, 234505, doi:10.1063/1.2121687, 2005.Ansmann, A., Tesche, M., Seifert, P., Althausen, T., Engelmann, R., Fruntke, J., Wandinger, U., Mattis, I., and Müller,

D.: Evolution of the ice phase in tropical altocumulus: SAMUM lidar observations over Cape Verde, J. Geophys. Res., 114, D17208, doi:10.1029/2008JD011659, 2009.

Atkinson, J. D., Murray, B. J., Woodhouse, M. T., Whale, T. F., Baustian, K. J., Carlslaw, K. S., Dobbie, S., O'Sullivan, D., and Malkin, T. L.: The importance of feldspar for ice nucleation by mineral dust in mixed-phase clouds, Nature, 498, 355-358, 2013.

Attard, E., Yang, H., Delort, A.-M., Amato, P., Pöschl, U., Glaux, C., Koop, T., and Morris, C. E.: Effects of atmospheric conditions on ice nucleation activity of Pseudomonas, Atmos. Chem. Phys., 12, 10667-10677, doi:10.5194/acp-12-10667-2012, 2012.

Augustin-Bauditz, S., Wex, H., Kanter, S., Ebert, M., Stolz, F., Prager, A., Niedermeier, D., and Stratmann, F.: The immersion mode ice nucleation behavior of mineral dusts: A comparison of different pure and surface modified dusts, Geophys. Res. Lett., 41, 7375-7382, doi:10.1002/2014GL061317, 2014.

Bassett, D. R., Boucher, E. A., and Zettlemoyer, A. C.: Adsorption studies on ice-nucleating substrates. Hydrophobed silicas and silver iodide, J. Colloid Interfac. Sci., 34, 436-446, 1970.

Christner, B. C.: Bioprospecting for microbial products that affect ice crystal formation and growth, Appl. Microbiol. Biotech., 85, 481-489, 2010.

Corrin, M. L., Edwards, H. W., and Nelson, J. A.: The surface chemistry of condensation nuclei: II. The preparation of silver iodide free of hygroscopic impurities and its interaction with water vapor, J. Atmos. Sci, 21, 565-567, 1964.

Darden, T., York, D., and Pedersen, L.: Particle mesh Ewald: An N·log(N) method for Ewald sums in large systems, J. Chem. Phys., 98, 10089-10092, doi:10.1063/1.464397, 1993.

de Boer, G., Morrison, H., Shupe, M. D., and Hildner, R.: Evidence of liquid dependent ice nucleation in high-latitude stratiform clouds from surface remote sensors, Geophys. Res. Lett., 38, L01803, doi:10.1029/2010GL046016, 2011.

Diehl, K., Quick, C., Matthias-Maser, S., Mitra, S. K., and Jaenicke, R.: The ice nucleation ability of pollen Part I: Laboratory studies in deposition and condensation freezing modes, Atmos. Res., 58, 75-87, 2001.

Diehl, K., Matthias-Maser, S., Jaenicke, R., and Mitra, S.K.: The ice nucleation ability of pollen

Part II. Laboratory studies in immersion and contact freezing modes, Atmos. Res., 61, 125-133, 2002.

Duman, J. G., Wu, D. W., Yeung, K. L., and Wolf, E. E.: Hemolymph proteins involved in the cold tolerance of terrestrial arthropods: antifreeze and ice nucleator proteins, Water and Life, Springer Berlin Heidelberg, ISBN-13: 9783540541127, 282-300, 1992.

Edwards, G. R., Evans, L. F., and La Mer, V. K.: Ice nucleation by monodisperse silver iodide particles, J. Colloid Sci., 17, 749-758, doi:10.1016/0095-8522(62)90049-1, 1962.

Fukuta, N.: Experimental studies of organic ice nuclei, J. Atmos. Sci., 23, 191-196, 1966.

Fukuta, N., and Schaller, R.C.: Ice nucleation by aerosol particles: Theory of condensation-freezing nucleation, J. Atmos. Sci., 39, 648-655, 1982.

Huber, R. G., Fuchs, J. E., von Grafenstein, S., Laner, M., Wallnoefer, H. G., Abdelkader, N., and Liedl, K. R.: Entropy from state probabilities: hydration entropy of cations, J. Phys. Chem. B, 117, 6466-6472, doi:10.1021/jp311418q, 2013.

Katz, U.: Wolkenkammeruntersuchungen der Eiskeimbildungsaktivität einiger ausgewählter Stoffe, Zeitschr. Angew. Math. Phys., 13, 333-358, 1962. (in German)

Kieft, T. L., and Ahmadjian, V: Biological ice nucleation activity in lichen mycobionts and photobionts, Lichenol.,21, 355-362, 1989.

Knopf, D. A., and Alpert, P. A.: A water activity based model of heterogeneous ice nucleation kinetics for freezing of water and aqueous solution droplets, Faraday Discuss., 165, 513-534, doi:10.1039/c3fd00035d, 2013.

Koop, T., Luo, B., Tsias, A., and Peter, T.: Water activity as the determinant for homogeneous ice nucleation in aqueous solutions, Nature, 406, 611-614, 2000.

Koop, T., and Zobrist, B.: Parameterizations for ice nucleation in biological and atmospheric systems, Phys. Chem. Chem. Phys., 11, 10741-11064, doi:10.1039/b914289d, 2009.

Krog, J. O., Zachariassen, K. E., Larsen, B., and Smidsrod, O.: Thermal buffering in Afro-alpine plants due to nucleating agent-induced water freezing, Nature, 282, 300-301, doi:10.1038/282300a0, 1979.

Lindow, S.E., Amy, D.C., and Upper, C.D.: Bacterial ice nucleation - a factor in frost injury to

plants, Plant Physiol., 70, 1084-1089, 1982.

Liou, Y.C., Tocilj, A., Davies, P.L., and Jia, Z.: Mimicry of ice structure by surface hydroxyls and water of a β-helix antifreeze protein, Nature, 406, 322-325, 2000.

Lundheim, R.: Physiological and ecological significance of biological ice nucleators, Phil. Trans. R. Soc. Lond. B., 357, 937-943, doi:10.1098/rstb.2002.1082, 2002.

Morris, C. E., Sands, D. C., Vinatzer, B. A., Glaux, C., Guilbaud, C., Buffière, A., Yan, S., Dominguez, H., and Thompson, B. M.: The life history of the plant pathogen Pseudomonas syringae is linked to the water cycle, ISME Journal, 2, 321-334, 2008.

Morris, C. E., Sands, D. C., Glaux, C., Samsatly, J., Asaad, S., Moukahel, A. R., Goncalves, F. I. T., and Bigg, K. E.: Urediospores of rust fungi are ice nucleation active at > –10°C and harbor ice nucleation active bacteria, Atmos. Chem. Phys., 13, 4223-4233, 2013a.

Morris, C. E., Monteil, C. L., and Berge, O.: The life history of Pseudomonas syringae: linking agriculture to Earth system processes, Annu. Rev. Phytopathol., 51, 85-104, 2013b.

Morris, C. E., Conen, F., Huffman, J. A., Phillips, V., Pöschl, U., and Sands, D. C: Bioprecipitation: A feedback cycle linking Earth history, ecosystem dynamics and land use through biological ice nucleators in the atmosphere, Global Change Biol., 20, 341-351, 2014.

Murray, B. J., O'Sullivan, D., Atkinson, J. D., Webb, M. E.: Ice nucleation by particles immersed in supercooled cloud droplets, Chem. Soc. Rev., 41, 6519-6554, 2012.

Osborne, T.B.: Die Pflanzenproteine, Ergebnisse der Physiologie, 10, 47-215, 1910. (in German)

Schnell, R., and Vali, G.: Biogenic ice nuclei part I: Terrestrial and marine sources, J. Atmos. Sci., 33, 1554-1564, 1976.

Shen J. H., Klier, K., and Zettlemoyer A. C.: Ice nucleation by micas, J. Atmos. Sci., 34, 957-960, 1977.

Staudinger, H., and Staudinger, M.: Die makromolekulare Chemie und ihre Bedeutung für die Protoplasmaforschung; in Protoplasmatologia, 1, 1, 2-6, Springer-Verlag Wien GmbH, doi:10.1007/978-3-7091-2448-2, 1954.

Steele, R.L., and Krebs, F.W.: Characteristics of silver iodide ice nuclei origination from anhydrous ammonia-silver iodide complexes, part I, J. Appl. Meteorol., 6.1, 1966.

Wallnoefer, H. G., Handschuh, S., Liedl, K. R., and Fox, T.: Stabilizing of a globular protein by a highly complex water network: a molecular dynamics simulation study on factor Xa, J. Phys. Chem. B, 114, 7405-7412, doi:10.1021/jp101654g, 2010.

Wex, H., DeMott, P. J., Tobo, Y., Hartmann, S., Rösch, M., Clauss, T., Tomsche, L., Niedermeier, D., and Stratmann, F.: Kaolinite particles as ice nuclei: learning from the use of different kaolinite samples and different coatings, Atmos. Chem. Phys., 14, 5529-5546, doi:10.5194/acp-14-5529-2014, 2014.

Wiacek, A., Peter, T., and Lohmann, U.: The potential influence of Asian and African mineral dust on ice, mixed-phase and liquid water clouds, Atmos. Chem. Phys., 10, 8649-8667, doi:10.5194/acp-10-8649-2010, 2010.

Zachariassen, K. E., and Kristiansen, E.: Ice nucleation and antinucleation in nature, Cryobiol., 41, 257-279, 2000.

Zobrist, B., Marcolli, C., Peter, T., and Koop, T.: Heterogeneous ice nucleation in aqueous solutions: the role of water activity, J. Phys. Chem. A, 112, 3965-3975, 2008.

Zolles, T., Burkart, J., Häusler, T., Pummer, B., Hitzenberger, R., and Grothe, H.: Identification of ice nucleation active sites on feldspar dust particles, J. Phys. Chem. A, *accepted*, doi:10.1021/jp509839x, 2015.

Elution time [min]	Mass range [kDa]
2.8–3.5	335–860
3.5–4.5	50–335
4.5–5.2	13–50
5.2–6.0	5–13
6.0–7.5	<5

Table S1: Sample fractions collected for INA tests and corresponding approximate molecular weights as estimated by calibration with standards. Although all fractions contained INMs, the first fraction contained the highest number concentration.

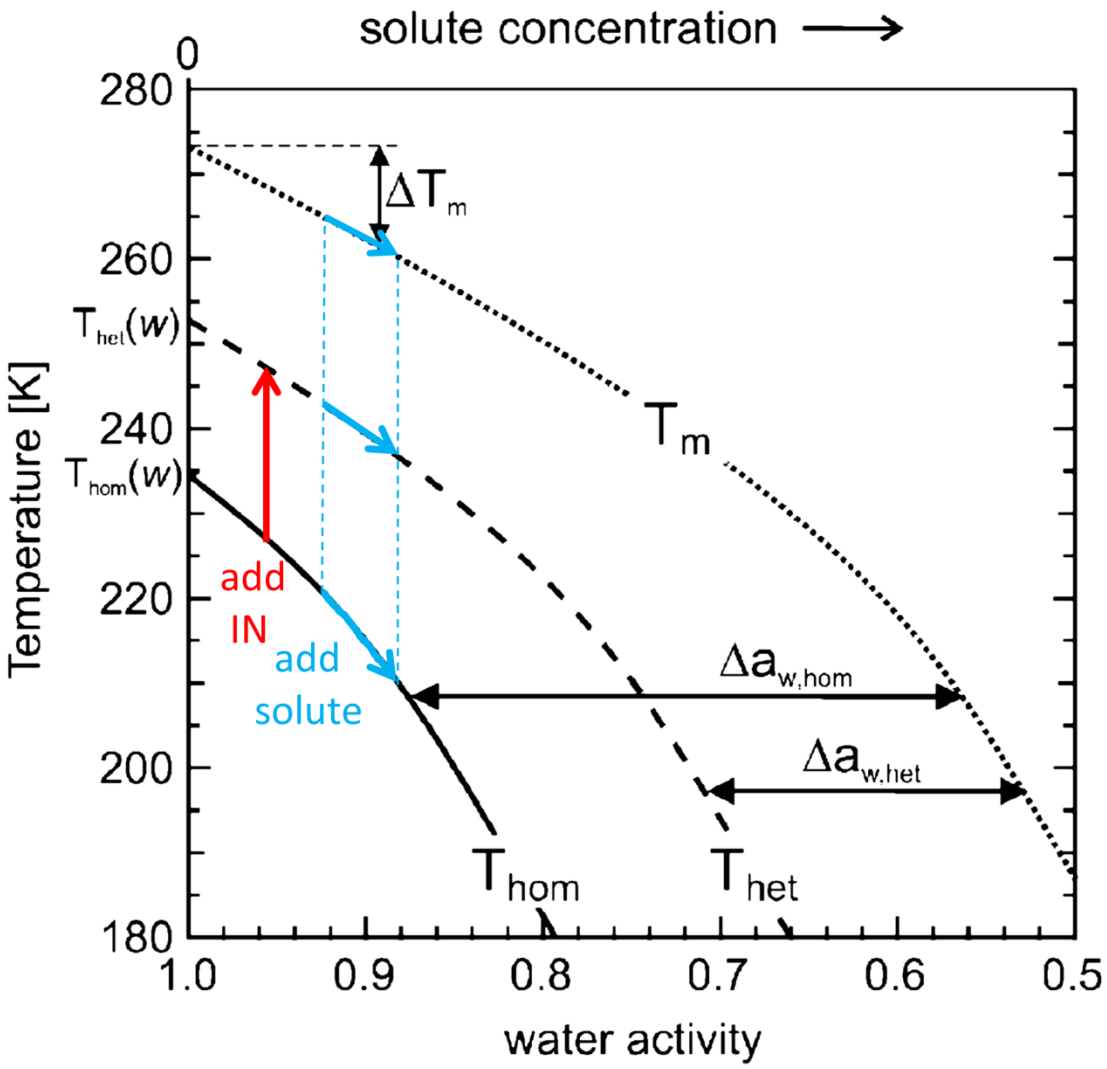

Figure S1: Correlation between a_w and T, based on Koop and Zobrist (2009). The vectors show the impact of INs (red) and freezing point depressing solutes (blue).